Remote sensing of forest diversities: The effect of image resolution and spectral plot extent

Lea Végh[1] ORCID iD: https://orcid.org/0000-0001-7948-480X

Shiro Tsuyuzaki[1] ORCID iD: https://orcid.org/0000-0003-3010-8699

[1]*Graduate School of Environmental Science, Hokkaido University, Japan*

Correspondence

Lea Végh, Graduate School of Environmental Science, Hokkaido University, N10 W5, Sapporo, Japan, 060-0810

Email: vegh@eis.hokudai.ac.jp

Abstract

Detecting field diversities via remote sensing is becoming important to monitor vegetation dynamics at large scale. The characteristics of the remotely sensed image, depending on the study organism and habitat, affect the efficiency of measuring α-and β-diversities. Therefore, we examined the impact of image resolutions and spectral plot extents on the accuracy of estimating forest α-diversities and compositional variances on the active volcano Mount Usu, northern Japan. Low (3.2 m) and high (0.8 m) resolution IKONOS multispectral images were used to create spectral indicators from pixels covering the field plots (narrow extent) and from pixels including neighbouring area (wide extent). Six forest diversity indices were obtained for canopy and for canopy-herb layer (total diversity): species richness (*S*), Shannon (*H*'), evenness (*J*'), Gini-Simpson (*D*), and true diversity of order 1 (N_1 = exp*H*') and order 2 (N_2 = *1/D*). Changes in species composition were assessed by dissimilarity matrices. The spectral diversity indicators were calculated from the combination of image resolutions and spectral plot extents, and then compared with field diversities. The low resolution–narrow extent based spectral indicators showed the highest correlations with canopy and total diversities. The best spectral indicators were derived from the scores of the first axis of principal component analysis and from the near infrared band, reaching high correlations with both canopy and total field diversity indices. Of the six field diversities, *J*' showed the highest correlations with single spectral indicators and $N_{1, 2}$

showed the highest correlations with pairs of spectral indicators. The correlations between spectral and field dissimilarities were lower than the correlations between α-diversities and spectral indicators, and were unaffected by the resolution and extent. In conclusion, the best spectral indicators were obtained from the low resolution–narrow extent combination, and the indicators estimated canopy and total field diversity indices of temperate forests equally.

1. Introduction

Monitoring diversity by field surveys (field diversity) is important to conserve vegetation and to identify biodiversity hotspots. α-diversity (community or plot diversity) is typically measured by establishing plots, but field surveys are time-consuming and often limited to a small number of samples. If plot diversity and compositional variations were estimated prior to the field surveys, monitoring could be better focused on the area of interest. Remote sensing shows potential to assess field diversities on large scales after validation, and is increasingly studied to complement field surveys.

Remotely sensed images have been applied for mapping habitats and species via evaluating spectral diversity measures (Wang and Gamon 2019): high resolution image analysis can accurately recognize species (Clark, Roberts, and Clark 2005; Underwood, Ustin, and DiPietro 2003) or estimate functional diversity (Huemmrich et al. 2013; Zomer, Trabucco, and Ustin 2009). Diversity is estimated by measuring the spectral heterogeneity of pixels; greater heterogeneity assumes greater heterogeneity within an area (Palmer et al., 2002). This is called the spectral variation hypothesis (SVH), which predicts that heterogeneous surfaces lead to increased richness, so increased spectral heterogeneity reflects increased diversity.

Most spectral diversity indicators are derived from single bands (Hall et al. 2012), vegetation indices (Gould 2000; Levin et al. 2007), or integrating multiple bands by principal component analysis (PCA) (Stickler and Southworth 2008). Common indicators are expressed by the mean, standard deviation (SD), or the coefficient of variation (CV) of the pixel values overlaying the field plots (Wang, Gamon, Cavender-Bares, et al. 2018). The accuracy of remotely sensed diversities varies due to the large range of landscapes and plant life forms. To increase the accuracy of diversity predictions, a present challenge is to identify

the source image requirements (Paganini et al. 2016) and a common set of habitat specific spectral diversity indicators (Skidmore et al. 2015). Therefore, the efficiency of spectral diversities should be tested on a wide range of environments using different source images to identify suitable community-specific indicators. Spectral indicators follow not only α-diversities, but also species compositional variations among plots (Feilhauer et al. 2013; Laliberté, Schweiger, and Legendre 2020). The methods used to detect changes in species composition range from ordination approaches by dissimilarity matrices (Cayuela et al. 2006) to applying Rao's Q (Rocchini et al. 2018; Botta-Dukát 2005).

Image characteristics vary with the sensor, and images need to be selected to suit the species being studied. If the resolution of the image is too fine compared to the species, the spectral diversities will be sensitive to within-target variance and overestimate spatial heterogeneity, while coarse resolution images will be insensitive to among-target variance and will underestimate heterogeneity (Rocchini et al. 2010; Woodcock and Strahler 1987). The spectral plot area covered by the pixels (hereafter, extent) from which the diversities are calculated also affects the relationship between field and spectral diversities (Figure 1); the inclusion of pixels surrounding the plot increases the accuracy of field diversity estimation (Parviainen, Luoto, and Heikkinen 2009). However, few studies examined the effects of including neighbouring pixels on spectral indicators, so their impact on evaluating field indices is unclear. Estimating total forest diversity (herb layer incorporated) has been also rarely examined, even though total diversity may be estimated with equal or higher accuracy than canopy diversity (Hakkenberg et al. 2018).

To confirm the effects of image resolution and different spectral plot extents on estimating field diversities, and to examine whether incorporating herb layer diversity in forest diversity increases the accuracy of the estimation, we created four different set of spectral diversity indicators from an IKONOS image covering temperate forests on Mount

Usu, Japan. Because the estimation accuracy also depends on the field diversity indices used to survey plots (Schmidtlein and Fassnacht 2017), we calculated six field indices for canopy only and for total diversity. Our major aim was to clarify the effects of resolution and spectral plot extent on the spectral diversities when estimating canopy and total diversities measured in the field. [Figure 1 position]

2. Methods

2.1. Image processing and plot selection

The study site, Mount Usu (42°32'N, 140°50'E), is an active volcano in the temperate region of northern Japan. Mount Usu erupted in every 20–30 years at different locations in the past century. Because the eruptions occurred at different locations, there are various forest types and transplantations differing in age on the mountain. As a result, the area is suitable to examine the performance of spectral diversity indicators in diverse forest types.

The IKONOS satellite image was taken on 1 August 2014 (wavelengths of bands: Blue 0.45–0.53 µm, Green 0.52–0.61 µm, Red 0.64–0.72 µm, Near-infrared (NIR) 0.76–0.86 µm, off-nadir: 19.27°), and was orthorectified using the Digital Elevation Model provided by the Geospatial Information Authority of Japan (accuracy within 0.7 m, resolution 6.2 m). After the orthorectification, the image was aligned to reference coordinates measured by portable GPS (Garmin GPSMAP 60CSx, accuracy ± 3 m) using second order polynomial transformation. The digital numbers were converted to surface reflectance by the dark-object subtraction method (Chavez 1988) and IKONOS correction factors (Taylor 2009), and pan-sharpening was done using the Brovey method (A. R. Gillespie, Kahle, and Walker 1986). All image processing was done by ArcGIS (ver. 10.2, ESRI).

A total of 35 plots measuring 10 m × 10 m were selected using stratified random sampling in the areas destroyed by the 1910 and 1977-78 eruptions (Figure 2). Of the 35

plots, 20 plots were established in young forests (less than 40 years old, 5 plots in closed- and 5 plots in open-canopy broadleaved forests, 5 plots in a *Picea* spp. plantation and 5 plots in a semi-artificial broadleaved forest) and 15 plots were established in mature forests (5 plots in an around 100 years old broadleaved forest, 5 plots in 70 years old and 5 plots in a 50 years old *Abies* spp. plantation, Supplemental material Figure S1). The mature forest plots were located at approximately 300 meters lower elevation than the young forest plots. The plots were established and located with GPS. [Figure 2 position]

2.2. Field survey and diversity indices

The field surveys in the 35 plots were conducted between 2015 and 2019, one to five years later than the satellite image was taken. Similar gaps between image acquisition and field survey did not cause problems in other studies (Levin et al. 2007; Warren et al. 2014), and field observations confirmed that the plots did not receive severe damages during this period. Canopy diversity was calculated from the number of stems on each tree species with a DBH above 3 cm (range: 3–67 cm) in 2016. In 15 plots, the survey covered 5 m × 5 m plots in 2016, and the plots were extended to 10 m × 10 m in 2019. In five of these plots, all of which were transplantations, trees fell due to a typhoon in the late summer of 2016. The fallen trees were left in the forest and were identified; therefore the forest structure of the plots could be reconstructed to 2014 canopy conditions. Herb layer diversity was measured in four 1 m × 1 m subplots within the plots during 2016 (before the typhoon) by counting the number of aboveground shoots rooted inside the subplots on each species shorter than 2 m in height.

Species richness (S), Shannon's entropy (H'), Gini-Simpson concentration (D), Shannon's evenness (J'), true diversity of order 1 (N_1) and true diversity of order 2 (N_2) were calculated for each plot by *vegan* (Oksanen et al. 2019) and *simba* (Jurasinski and Retzer 2012) packages of the R software (R Core Team 2018). The equations are:

S = number of species in a given plot, (1)

$H' = -\sum_{i=1}^{s} p_i \ln p_i$, (2)

$J' = H'/\log S$ (3)

$D = 1 - \sum_{i=1}^{s} p_i^2$, (4)

$N_1 = \exp H'$, (5)

$N_2 = 1/D$, (6)

,where p_i is the relative dominance of ith species in a given plot. These indices were chosen to include popular indices like species richness (Carlson et al. 2007; Rocchini, Ricotta, and Chiarucci 2007; Viedma et al. 2012), and the Shannon entropy (Oldeland et al. 2010; Wang, Gamon, Cavender-Bares, et al. 2018), and the relatively untested true diversities, which are argued to be better suited to describe diversity and compare studies (Jost 2006; Tuomisto 2010). Two sets of field diversities were calculated: canopy diversity and total diversity, the latter being the average of canopy and herb layer diversity. Variation in species composition between plots was evaluated by Bray-Curtis dissimilarity matrices by presence/absence (i.e., Sørensen index) and by abundance of species (Oksanen et al. 2019).

2.3. Spectral diversity indicators

To test the effects of resolution on the spectral diversity indicators, the indicators were calculated from low (3.2 m) and high resolution (0.8 m) images. The impact of neighbouring pixels on spectral diversities was examined by using two spectral plot extents (Figure 1); the narrow extent covered pixels corresponding to the field plots (10 m × 10 m square), while the wide extent included additional neighbouring pixels (10 m radius circle centred in the plot). For the low resolution, the number of pixels per plot ranged between 9–12 (narrow extent)

and 28–32 (wide extent), and for the high resolution ranged between 144–169 (narrow extent) and 472–480 (wide extent). Within the high resolution spectral plots, in average 5% of the pixels were in shadow for narrow extent (range 1–15%) and 3% for wide extent (range 0–12%). Excluding shaded pixels did not change the correlations between single spectral indicators and field indices (Kruskal-test, $P = 0.21$), although the regressions were slightly increased when two spectral indicators were used as explanatory variables (Kruskal-test, $P = 0.02$). However, the best regression pairs remained the same; therefore, we retained the shaded pixels in the high resolution spectral plots to cover the same areas as the low resolution spectral plots.

The reflectance values of the four bands, Blue, Green, Red, and NIR, and the Normalized difference vegetation index (NDVI, calculated as (NIR – Red) / (NIR + Red); Rouse et al., 1974) were recorded for every pixel at each resolution and extent combination and were imported to R software. Using the four bands as a matrix, PCA was carried out (Rocchini, Ricotta, and Chiarucci 2007): the first principal component (PC1) explained more than 99% of the variation in the bands and was included for calculating spectral diversities.

The first set of spectral diversities was calculated by taking the mean, range (difference between minimum and maximum values), SD, and CV of each band, NDVI, and PC1 by plot for the four combinations of resolutions and extents. In addition, the mean Euclidean distance (Distance) from the plot centre was calculated using the bands as coordinate system axis (Rocchini, Ricotta, and Chiarucci 2007; Schmidtlein and Fassnacht 2017).

The second set of spectral diversities was calculated by counting the unique reflectance values as species and calculating the same diversity indices as from field observations: if three and six pixels out of nine had the same values, then the richness (marked by bold $\boldsymbol{S}$ to distinguish from field diversity S) of the spectral plot was regarded as

two. NDVI and PC1 values were sorted into 40 equal sized bins and the bins were handled afterwards as unique values. In total, 63 spectral indicators were calculated for each resolution and extent combinations (Table 1). Pairwise differences of the 63 spectral diversities were examined by the Euclidean distance matrices. [Table 1 position]

2.4. Comparison of the field diversity indices and spectral diversity indicators

Pearson's correlation coefficient (r) and linear regression models (LM) were used to investigate the relationship between the field indices and spectral indicators. From the six field diversity indices and 63 spectral indicators all together 3024 correlations were calculated for α-diversity ($6 \times 63 \times 4 \times 2$, for all combinations of field and spectral diversities, resolutions, extents, and field layers) and 504 dissimilarity matrices of species composition ($63 \times 4 \times 2$). Correlations with a P value of less than 0.05 were treated as strong correlations. Significant differences in the number of strong correlations between low and high resolutions and between narrow and wide extents were examined by χ^2-test. The effects of resolution, extent, and elevation on the correlation coefficients were examined by non-parametric Kruskal-Wallis test and pairwise Wilcoxon test.

We applied stepwise multiple regression analysis to test the predictability of field diversities by one to five spectral indicators as explanatory variables using the R package *leaps* (Miller, 2020). LM was used to examine more in detail the accuracy when the number of explanatory variables was limited to two spectral indicators, testing all combination of pairs. We retained those models, where all coefficients were significant at $P < 0.05$, to identify spectral indicator pairs estimating field indices with high accuracy. The effects of elevation on field indices and spectral indicators were examined with LM, using elevation alone and paired with spectral diversities as explanatory variable. In addition, spatial auto-correlation of field and spectral diversities was tested by Moran's I (Moran 1950).

The significance of correlations between the dissimilarity matrices of field diversity indices and spectral diversity indicators were determined by Mantel-test with ten thousand permutations (Mantel 1967; Legendre and Legendre 2012). The dissimilarity of the seven forest types based on age and species composition was measured with ANOSIM and the *P* value was calculated by ten thousand permutations (Clarke 1993).

3. Results

3.1. The effects of resolution and extent on correlations

The number of strong correlations, where *P* was less than 0.05, was low and changed with resolution and spectral plot extent (Table 2). The spectral indicators derived from low resolution had a higher number of strong correlations, both with canopy and total diversities, than those derived from high resolution (χ^2-test, $P < 0.001$). The number of strong correlations increased when narrow extent was used ($P < 0.001$ against canopy and $P = 0.02$ against total indices). Canopy diversities had a higher number of strong correlations than total diversities ($P < 0.001$), but their range was the same, i.e., *r* ranging 0.34 – 0.50 with canopy and 0.33 – 0.50 with total indices (in absolute values, Kruskal-Wallis test, $P = 0.87$). The highest correlations were obtained from the low resolution–narrow extent spectral indicators (Table 2), both in the case of canopy ($r = 0.50$, *J'* – PC1-***D***) and total diversities ($r = 0.50$, *J'* – PC1-***H'***). The other resolution–extent combinations had significantly lower correlations with canopy diversities (Figure 3*a*, $P \leq 0.03$), while with total diversities only the high resolution–wide extent based spectral indicators had significantly higher correlations ($P = 0.04$). [Table 2 position]

3.2. The impacts of field indices and spectral indicators

From the field diversity indices, the canopy N_1 and N_2 yielded the highest number of strong

correlations with spectral indicators (18 and 16 cases), while from the total indices, *D* had the highest number of strong correlations (15 cases). However, the number of correlations did not indicate strong relationship; field *J'* produced the highest *r* (Figure 3*b*) significantly outperforming other field indices (canopy: Wilcoxon test, $P < 0.001$, total: Kruskal-Wallis test, $P < 0.01$). Most field indices showed high correlation with multiple spectral indicators, but total $N_{1,2}$ and *H'* correlated only with high resolution–wide extent Blue-***J'***. [Figure 3 position]

Across all resolutions and extents, 20 and 15 spectral indicators were correlated significantly with canopy and total diversity indices. Most spectral indicators displayed strong correlations at low resolution–narrow extent combination (Figure 4), and were mostly calculated from NIR, NDVI, and PC1 scores. PC1-based spectral indicators had high correlations with both canopy and total field diversities, while NIR and NDVI based indicators were correlated stronger with canopy indices. From the PC1 indicators, SD and range were best with canopy indices, while PC1 indicators calculated as ***S***, ***D***, ***H'***, $\boldsymbol{N_{1,2}}$ were correlated stronger with total *J'* and *D*. The highest correlations for each combination were positive among the field and spectral diversities, apart from the spectral indicators PC1-CV and Blue-***J'***, which displayed negative correlations (Figure 5). [Figure 4 and 5 position]

3.3. Linear relationships between field indices and spectral indicators

The best predictor variables identified by stepwise regression analysis changed with resolution, extent and the maximum number of predictors, although spectral indicators based on the Blue band and NDVI were kept often in the final regression models. To keep the number of variables low, we concentrated on models with two explanatory variables (pairs of spectral indicators).

The resolution and extent did not affect the number of significant regressions when estimating total diversity indices (χ^2-test, $P = 0.96$ and $P = 0.28$), but regression models using low resolution–narrow extent based spectral indicator pairs fitted better than models using low–wide and high–narrow based spectral indicators (Wilcoxon test, $P < 0.01$, Figure 6*a*). When predicting canopy diversities, low resolution (χ^2-test, $P < 0.001$) and wide extent ($P < 0.001$) spectral indicator pairs had higher number of significant regressions. The explained variance also increased when low resolution–wide extent spectral diversity pairs were used to estimate canopy diversity indices (Wilcoxon test, $P < 0.01$). Canopy N_1 ($P < 0.05$) and total D ($P < 0.01$) displayed larger average r than the other field indices (Figure 6*b*), while total H' had generally lower r than other field indices ($P < 0.01$). The explained variance was highest when spectral indicator pairs were derived from low resolution and narrow extent (Figure 7). Namely, the pair of Blue-SD and Blue-range predicted canopy N_1 (LM, $r = 0.64$, $P < 0.001$) and the pair of Red-***D*** and PC1-***D*** predicted total J' ($r = 0.61$, $P = 0.02$). Significant regressions against canopy indices were fewer (χ^2-test, $P < 0.001$), but stronger than regressions against total indices (Kruskal-Wallis test, $P < 0.001$). [Figure 6 and 7 position]

3.4. Effects of elevation and spatial autocorrelation

Field indices S, H', and $N_{1,2}$ correlated negatively with the elevation when all 35 plots were analysed together ($r = -0.37$ to -0.52, $P < 0.05$). However, when the higher elevation young forest and lower elevation mature forest plots were analysed separately, the elevation of plots did not affect the field diversities. Pairing elevation with spectral diversity indicators as explanatory variable in regression models improved the fit of the models in the case of two and thirteen spectral indicators when regressing against canopy and total diversities, respectively. The highest r was reached when estimating canopy N_1 and elevation was paired with NDVI-mean ($r = 0.65$), and when estimating total H' with elevation paired with Blue-***J'***

(r = 0.64).

The canopy and total diversity indices displayed different spatial-autocorrelation patterns. Of the canopy diversities, only *J'* showed spatial-autocorrelation (I = 0.12, P = 0.02), while all total indices were spatially auto-correlated except for *D*. The spectral indicators showing the highest correlations with canopy diversities did not show autocorrelation when calculated from high resolution but did show when calculated from low resolution–narrow extent (P = 0.01). As for the best spectral indicators correlating with total diversities, only the Blue-***J'*** calculated from high–wide combination showed spatial autocorrelation (P < 0.001). In general, spectral indicators calculated via SD, mean, CV, and range showed autocorrelation.

3.5. Changes in species composition

The Bray-Curtis matrices by species abundance correlated better with the spectral matrices than the matrices by presence/absence, so the analyses by abundance matrices were described. The dissimilarity matrices of species composition and spectral diversity indicators did not show as high correlations as α-diversity indices did with spectral indicators. The dissimilarity matrix of canopy species composition had more strong correlations with the spectral indicators than the total species matrix (χ^2-test, P < 0.001) and showed the highest correlation coefficient with PC1-mean from low resolution–wide extent image (Mantel's r = 0.36). Correlations with the total matrix were higher compared to the canopy matrix (Kruskal-Wallis test, P < 0.004), but the highest correlation—reached with low–narrow Red-***J'***, r = 0.32—was below that of the canopy. The canopy matrix had more significant correlations with high resolution spectral matrices (χ^2-test, P = 0.01), while the total matrix had more correlations with low resolution matrices (P = 0.03). Neither the combinations of

resolutions and extents, nor the selection of spectral indicators when calculating the dissimilarity matrices affected the strength of the correlations, however.

In spite of the relatively low correlations between field and spectral matrices, the spectral indicators distinguished between the forest types (ANOSIM, canopy composition: $r = 0.55$, total composition: $r = 0.36$) and between old and young forests in the case of canopy composition ($r = 0.52$, Supplemental material Figure S2, Table S1).

4. Discussion

4.1. The effects of resolution and extent

The resolution and inclusion of neighbouring pixels affected the correlations and regressions between spectral and field diversities. The effects depended on the choice of field indices and whether canopy or total diversities were evaluated.

The low and high resolution images used in this study had relatively fine resolution. Other studies report high correlations with species richness using either Quickbird (resolution same as the low resolution used here) or Landsat images (30 m resolution) in wetlands (Rocchini 2007) and mountain forests (Levin et al. 2007). However, examples exist where similar fine resolution images (resolution same as the high resolution used here) are found to have too fine spatial resolution to observe canopy richness (Nagendra et al. 2010). This study demonstrated that low resolution spectral indicators showed higher Pearson's correlation coefficients with field diversity indices. This suggests that the high resolution diversities reflected within study object heterogeneity which decreased their accuracy (Wang and Gamon 2019; Woodcock and Strahler 1987).

Increasing the pixel number per plot, i.e., wide extent, did not improve the correlations if single spectral indicators were used, and had inconsistent effect when pairs of spectral indicators were used. However, the wide extent had an advantage to calculate unique

value based spectral indicators, as the low resolution–narrow extent based spectral plots often had too few pixels and displayed perfect evenness (all values were unique). Although calculating spectral indicators from as few as nine pixels is not rare (Madonsela et al. 2017; Torresani et al. 2019; Woodcock and Strahler 1987), in those cases the indicators are based on measuring variance via traditional methods (e.g. mean, SD, or CV). Spectral indicators that strongly correlated with field indices, i.e., PC1, NDVI, and NIR, did not suffer from the problem of low pixel number, so the neighbouring pixels had no positive impact on them. The present study measured field diversities from one plot shape, but plot shape influences field measurements of diversities (Korb, Covington, and Fulé 2003; Marignani, Del Vico, and Maccherini 2007). Experimenting with multiple plot shapes and corresponding spectral extents when calculating indicators may find that plot shapes influence the performance of spectral indicators.

4.2. The effects of field indices and including herb diversity

Spectral indicators showed the highest correlations with *J'* when single spectral indicator was used, and with N_1 and N_2 when pairs of spectral indicators were used. Although the spectral diversities were correlated differently with canopy and total diversities, high correlations were observed with both canopy and total field indices. Recent studies on the correlation of field and spectral indices are often using *H'* or *D* (Oldeland et al. 2010; Wang, Gamon, Schweiger, et al. 2018), as these indices incorporate information about the abundance of species and were shown to correlate stronger with spectral diversities than *S*, which only measures presence/absence (Underwood, Ustin, and DiPietro 2003). We observed low correlations between spectral indicators and *S*, but found that *J'* and $N_{1,2}$ showed higher correlations with spectral indicators than *H'* and *D*, especially when estimating canopy diversities. Abundance-based dissimilarity matrices also displayed higher correlations than

presence/absence-based matrices when estimating compositional variations of species, supporting the importance of abundance sensitive diversity measures.

The best spectral indicators correlating with field diversities were obtained from low resolution images, although high resolution–wide extent indicators estimated total diversities well. When the study organism is large, using low resolution images for calculating spectral diversities increases the accuracy (Stickler and Southworth 2008). Conversely, spectral indicators based on high resolution images can observe small size organism, such as ant colonies (Lassau et al. 2005). These suggest that high resolution images are better to estimate total forest diversity because small plants need to be detected as well. In this study, the total diversity was evaluated well both by low resolution–narrow extent and high resolution–wide extent based spectral indicators, so the total indices seemed not to show a clear preference for high resolution images.

Combining spectral indicators estimates field diversities better than single spectral indicators in tropical dry forest (T. W. Gillespie 2005) and in central-African forest (Thenkabail et al. 2003). We also observed improvement when two spectral indicators were used to estimate field indices, especially, when assessing $N_{1,2}$. True diversities are rarely used and they display low performance compared to *H'* in Borneo tropical forests (Foody and Cutler 2003). Our results suggested that $N_{1,2}$ was sensitive to habitat differences when combined with remotely sensed indicators, estimating diversities in temperate forests more than in tropical forests.

4.3. Band specificity of spectral indicators

When correlating spectral indicators with canopy diversity indices, the best spectral indicators were derived from the PC1 and NIR. When correlating with total diversities, the best spectral indicators were derived from the PC1 and from mostly visible bands. Spectral

indicators derived from NDVI displayed weak correlations, possibly because NDVI is correlated with the productivity of plant communities rather than with the landscape heterogeneity (Johansen and Tømmervik 2014). Productivity is more related to canopy diversity than to total diversity because the biomass of trees is larger than the biomass of understorey plants (Zhang, Chen, and Taylor 2016). This is consistent with the fact that NDVI-based indices estimated the canopy diversities better than the total diversities. The high performance of PC1-based indicators showed that integrating multiple bands created the most successful spectral indicator source.

A limitation of the study is the use of single source image to calculate spectral diversities, as combining multiple satellite images from different dates are shown to increase the accuracy of spectral indicators (Dudley et al. 2015; Räsänen and Virtanen 2019). However, the image acquisition date was in the summer season, when the status of local vegetation was optimal for remote observation (Schmidtlein and Fassnacht 2017).

Conclusion

The spectral diversity indicators based on low resolution and narrow extent had higher correlations with the field indices. Spectral diversities based on PC1 and NIR had high correlations and using two spectral indicators estimated field diversities better. In particular, the canopy diversities were evaluated by the spectral diversities using PC1 and NIR, while the total diversities were evaluated using the PC1 and visible bands. Among the field diversities, J' and $N_{1,2}$ were estimated best. Although compositional changes in species were detected less then α-diversities, forest types were distinguished well. The present study confirmed that spectral indicators estimate canopy and total field diversities in various temperate forests. As canopy diversity is a good predictor of total forest diversity (Hakkenberg et al. 2018) and it is faster to survey, future studies should focus on it to

evaluate forest diversities.

Acknowledgements

The study was partly funded by the Japan Society for the Promotion of Science and Japan Aerospace Exploration Agency. We are grateful for the support of the Japanese Ministry of Education, Culture, Sports, Science and Technology. The authors declare that they have no conflict of interest.

References

Botta-Dukát, Zoltán. 2005. "Rao's Quadratic Entropy as a Measure of Functional Diversity Based on Multiple Traits." *Journal of Vegetation Science* 16 (5): 533–40. https://doi.org/10.1111/j.1654-1103.2005.tb02393.x.

Carlson, Kimberly M., Gregory P. Asner, R. Flint Hughes, Rebecca Ostertag, and Roberta E. Martin. 2007. "Hyperspectral Remote Sensing of Canopy Biodiversity in Hawaiian Lowland Rainforests." *Ecosystems* 10 (4): 536–49. https://doi.org/10.1007/s10021-007-9041-z.

Cayuela, Luis, José María Rey Benayas, Ana Justel, and Javier Salas-Rey. 2006. "Modelling Tree Diversity in a Highly Fragmented Tropical Montane Landscape." *Global Ecology and Biogeography* 15 (6): 602–13. https://doi.org/10.1111/j.1466-8238.2006.00255.x.

Chavez, Pat S. 1988. "An Improved Dark-Object Subtraction Technique for Atmospheric Scattering Correction of Multispectral Data." *Remote Sensing of Environment* 24 (3): 459–79. https://doi.org/10.1016/0034-4257(88)90019-3.

Clark, Matthew L., Dar A. Roberts, and David B. Clark. 2005. "Hyperspectral Discrimination of Tropical Rain Forest Tree Species at Leaf to Crown Scales." *Remote Sensing of Environment* 96 (3): 375–98. https://doi.org/10.1016/j.rse.2005.03.009.

Clarke, K. R. 1993. "Non-Parametric Multivariate Analyses of Changes in Community Structure." *Australian Journal of Ecology* 18 (1): 117–43. https://doi.org/10.1111/j.1442-9993.1993.tb00438.x.

Dudley, Kenneth L., Philip E. Dennison, Keely L. Roth, Dar A. Roberts, and Austin R. Coates. 2015. "A Multi-Temporal Spectral Library Approach for Mapping Vegetation Species across Spatial and Temporal Phenological Gradients." *Special Issue on the Hyperspectral Infrared Imager (HyspIRI)* 167 (September): 121–34. https://doi.org/10.1016/j.rse.2015.05.004.

Feilhauer, Hannes, Frank Thonfeld, Ulrike Faude, Kate S. He, Duccio Rocchini, and Sebastian Schmidtlein. 2013. "Assessing Floristic Composition with Multispectral Sensors—A Comparison Based on Monotemporal and Multiseasonal Field Spectra." *International Journal of Applied Earth Observation and Geoinformation* 21 (April): 218–29. https://doi.org/10.1016/j.jag.2012.09.002.

Foody, Giles M., and Mark E. J. Cutler. 2003. "Tree Biodiversity in Protected and Logged Bornean Tropical Rain Forests and Its Measurement by Satellite Remote Sensing." *Journal of Biogeography* 30 (7): 1053–66. https://doi.org/10.1046/j.1365-2699.2003.00887.x.

Gillespie, Alan R., Anne B. Kahle, and Richard E. Walker. 1986. "Color Enhancement of Highly Correlated Images. I. Decorrelation and HSI Contrast Stretches." *Remote Sensing of Environment* 20 (3): 209–35. https://doi.org/10.1016/0034-4257(86)90044-1.

Gillespie, Thomas W. 2005. "Predicting Woody-Plant Species Richness in Tropical Dry Forests: A Case Study from South Florida, USA." *Ecological Applications* 15 (1): 27–37. https://doi.org/10.1890/03-5304.

Gould, William. 2000. "Remote Sensing of Vegetation, Plant Species Richness, and Regional Biodiversitzy Hotspots." *Ecological Applications* 10 (6): 1861–70. https://doi.org/10.1890/1051-0761(2000)010[1861:RSOVPS]2.0.CO;2.

Hakkenberg, C. R., K. Zhu, R. K. Peet, and C. Song. 2018. "Mapping Multi-Scale Vascular Plant Richness in a Forest Landscape with Integrated LiDAR and Hyperspectral Remote-Sensing." *Ecology* 99 (2): 474–87. https://doi.org/10.1002/ecy.2109.

Hall, Karin, Triin Reitalu, Martin T. Sykes, and Honor C. Prentice. 2012. “Spectral Heterogeneity of QuickBird Satellite Data Is Related to Fine-Scale Plant Species Spatial Turnover in Semi-Natural Grasslands.” *Applied Vegetation Science* 15 (1): 145–57. https://doi.org/10.1111/j.1654-109X.2011.01143.x.

Huemmrich, K. F., J. A. Gamon, C. E. Tweedie, P. K. E. Campbell, D. R. Landis, and E. M. Middleton. 2013. “Arctic Tundra Vegetation Functional Types Based on Photosynthetic Physiology and Optical Properties.” *IEEE Journal of Selected Topics in Applied Earth Observations and Remote Sensing* 6 (2): 265–75. https://doi.org/10.1109/JSTARS.2013.2253446.

Johansen, Bernt, and Hans Tømmervik. 2014. “The Relationship between Phytomass, NDVI and Vegetation Communities on Svalbard.” *International Journal of Applied Earth Observation and Geoinformation* 27: 20–30. https://doi.org/10.1016/j.jag.2013.07.001.

Jost, Lou. 2006. “Entropy and Diversity.” *Oikos* 113 (2): 363–75.

Jurasinski, Gerald, and with contributions from Vroni Retzer. 2012. *Simba: A Collection of Functions for Similarity Analysis of Vegetation Data*. https://CRAN.R-project.org/package=simba.

Korb, Julie E., W. W. Covington, and Peter Z. Fulé. 2003. “Sampling Techniques Influence Understory Plant Trajectories After Restoration: An Example from Ponderosa Pine Restoration.” *Restoration Ecology* 11 (4): 504–15. https://doi.org/10.1046/j.1526-100X.2003.rec0170.x.

Laliberté, Etienne, Anna K. Schweiger, and Pierre Legendre. 2020. “Partitioning Plant Spectral Diversity into Alpha and Beta Components.” *Ecology Letters* 23 (2): 370–80. https://doi.org/10.1111/ele.13429.

Lassau, Scott A., Gerasimos Cassis, Paul K. J. Flemons, Lance Wilkie, and Dieter F. Hochuli. 2005. “Using High-Resolution Multi-Spectral Imagery to Estimate Habitat Complexity in Open-Canopy Forests: Can We Predict Ant Community Patterns?” *Ecography* 28 (4): 495–504. https://doi.org/10.1111/j.0906-7590.2005.04116.x.

Legendre, Pierre, and Louis Legendre. 2012. *Numerical Ecology*. 3rd English ed. Developments in Environmental Modelling 24. Amsterdam ; Tokyo: Elsevier.

Levin, Noam, Avi Shmida, Oded Levanoni, Hagit Tamari, and Salit Kark. 2007. “Predicting Mountain Plant Richness and Rarity from Space Using Satellite-Derived Vegetation Indices.” *Diversity and Distributions* 13 (6): 692–703. https://doi.org/10.1111/j.1472-4642.2007.00372.x.

Madonsela, Sabelo, Moses Azong Cho, Abel Ramoelo, and Onisimo Mutanga. 2017. “Remote Sensing of Species Diversity Using Landsat 8 Spectral Variables.” *ISPRS Journal of Photogrammetry and Remote Sensing* 133 (November): 116–27. https://doi.org/10.1016/j.isprsjprs.2017.10.008.

Mantel, Nathan. 1967. “The Detection of Disease Clustering and a Generalized Regression Approach.” *Cancer Research* 27 (2 Part 1): 209.

Marignani, Michela, Eva Del Vico, and Simona Maccherini. 2007. “Spatial Scale and Sampling Size Affect the Concordance between Remotely Sensed Information and Plant Community Discrimination in Restoration Monitoring.” *Biodiversity and Conservation* 16 (13): 3851–61. https://doi.org/10.1007/s10531-007-9184-4.

Miller, Thomas Lumley based on Fortran code by Alan. 2020. *Leaps: Regression Subset Selection*. https://CRAN.R-project.org/package=leaps.

Moran, P. A. P. 1950. “Notes on Continuous Stochastic Phenomena.” *Biometrika* 37 (1/2): 17–23. https://doi.org/10.2307/2332142.

Nagendra, Harini, Duccio Rocchini, R. Ghate, B. Sharma, and S. Pareeth. 2010. “Assessing Plant Diversity in a Dry Tropical Forest: Comparing the Utility of Landsat and Ikonos Satellite Images” 2 (2): 478–96. https://doi.org/10.3390/rs2020478.

Oksanen, Jari, F. Guillaume Blanchet, Michael Friendly, Roeland Kindt, Pierre Legendre, Dan McGlinn, Peter R. Minchin, et al. 2019. *Vegan: Community Ecology Package*. https://CRAN.R-project.org/package=vegan.

Oldeland, Jens, Dirk Wesuls, Duccio Rocchini, Michael Schmidt, and Norbert Jürgens. 2010. “Does Using Species Abundance Data Improve Estimates of Species Diversity from Remotely Sensed Spectral Heterogeneity?” *Ecological Indicators* 10 (2): 390–96. https://doi.org/10.1016/j.ecolind.2009.07.012.

Paganini, Marc, Allison K. Leidner, Gary Geller, Woody Turner, and Martin Wegmann. 2016. “The Role of Space Agencies in Remotely Sensed Essential Biodiversity Variables.” Edited by Harini Nagendra and Clement Atzberger. *Remote Sensing in Ecology and Conservation* 2 (3): 132–40. https://doi.org/10.1002/rse2.29.

Palmer, Michael W., Peter G. Earls, Bruce W. Hoagland, Peter S. White, and Thomas Wohlgemuth. 2002. “Quantitative Tools for Perfecting Species Lists.” *Environmetrics* 13 (2): 121–37. https://doi.org/10.1002/env.516.

Parviainen, Miia, Miska Luoto, and Risto K. Heikkinen. 2009. “The Role of Local and Landscape Level Measures of Greenness in Modelling Boreal Plant Species Richness.” *Ecological Modelling* 220 (20): 2690–2701. https://doi.org/10.1016/j.ecolmodel.2009.07.017.

R Core Team. 2018. *R: A Language and Environment for Statistical Computing* (version 3.5.1). Vienna, Austria: R Foundation for Statistical Computing. https://www.R-project.org/.

Räsänen, Aleksi, and Tarmo Virtanen. 2019. “Data and Resolution Requirements in Mapping Vegetation in Spatially Heterogeneous Landscapes.” *Remote Sensing of Environment* 230 (September): 111207. https://doi.org/10.1016/j.rse.2019.05.026.

Rocchini, Duccio. 2007. “Effects of Spatial and Spectral Resolution in Estimating Ecosystem α-Diversity by Satellite Imagery.” *Remote Sensing of Environment* 111 (4): 423–34. https://doi.org/10.1016/j.rse.2007.03.018.

Rocchini, Duccio, Niko Balkenhol, Gregory A. Carter, Giles M. Foody, Thomas W. Gillespie, Kate S. He, Salit Kark, et al. 2010. “Remotely Sensed Spectral Heterogeneity as a Proxy of Species Diversity: Recent Advances and Open Challenges.” *Ecological Informatics* 5 (5): 318–29. https://doi.org/10.1016/j.ecoinf.2010.06.001.

Rocchini, Duccio, Sandra Luque, Nathalie Pettorelli, Lucy Bastin, Daniel Doktor, Nicolò Faedi, Hannes Feilhauer, et al. 2018. “Measuring β-Diversity by Remote Sensing: A Challenge for Biodiversity Monitoring.” *Methods in Ecology and Evolution* 9 (8): 1787–98. https://doi.org/10.1111/2041-210X.12941.

Rocchini, Duccio, Carlo Ricotta, and A. Chiarucci. 2007. “Using Satellite Imagery to Assess Plant Species Richness: The Role of Multispectral Systems.” *Applied Vegetation Science* 10 (3): 325–31. https://doi.org/10.1111/j.1654-109X.2007.tb00431.x.

Rouse, J.W., R.H. Haas, J.A. Schell, and D.W. Deering. 1974. “Monitoring Vegetation Systems in the Great Plains with ERTS.” In *Proceedings of Third Earth Resources Technology Satellite-1 Symposium*, 1:48–62. Washington, DC, USA.

Schmidtlein, Sebastian, and Fabian Ewald Fassnacht. 2017. “The Spectral Variability Hypothesis Does Not Hold across Landscapes.” *Remote Sensing of Environment* 192 (April): 114–25. https://doi.org/10.1016/j.rse.2017.01.036.

Skidmore, A. K., Nathakie Pettorelli, Nicholas Coops, Gary Geller, Matthew Hansen, Richard Lucas, Caspar Muncher, et al. 2015. “Environmental Science : Agree on

Biodiversity Metrics to Track from Space." *Nature* 523 (7561): 403–5. https://doi.org/10.1038/523403a.
Stickler, Claudia M., and Jane Southworth. 2008. "Application of Multi-Scale Spatial and Spectral Analysis for Predicting Primate Occurrence and Habitat Associations in Kibale National Park, Uganda." *Remote Sensing of Environment* 112 (5): 2170–86. https://doi.org/10.1016/j.rse.2007.10.013.
Taylor, Martin. 2009. "IKONOS Planetary Reflectance and Mean Solar Exoatmospheric Irradiance," IKONOS Planetary Reflectance, QSOL Rev. 2, , 3.
Thenkabail, Prasad S, Jefferson Hall, Tiffany Lin, Mark S Ashton, David Harris, and Eden A Enclona. 2003. "Detecting Floristic Structure and Pattern across Topographic and Moisture Gradients in a Mixed Species Central African Forest Using IKONOS and Landsat-7 ETM+ Images." *International Journal of Applied Earth Observation and Geoinformation* 4 (3): 255–70. https://doi.org/10.1016/S0303-2434(03)00006-0.
Torresani, Michele, Duccio Rocchini, Ruth Sonnenschein, Marc Zebisch, Matteo Marcantonio, Carlo Ricotta, and Giustino Tonon. 2019. "Estimating Tree Species Diversity from Space in an Alpine Conifer Forest: The Rao's Q Diversity Index Meets the Spectral Variation Hypothesis." *Ecological Informatics* 52: 26–34. https://doi.org/10.1016/j.ecoinf.2019.04.001.
Tuomisto, Hanna. 2010. "A Consistent Terminology for Quantifying Species Diversity? Yes, It Does Exist." *Oecologia* 164 (4): 853–60. https://doi.org/10.1007/s00442-010-1812-0.
Underwood, Emma, Susan Ustin, and Deanne DiPietro. 2003. "Mapping Nonnative Plants Using Hyperspectral Imagery." *Remote Sensing of Environment* 86 (2): 150–61. https://doi.org/10.1016/S0034-4257(03)00096-8.
Viedma, Olga, Iván Torres, Beatriz Pérez, and José M. Moreno. 2012. "Modeling Plant Species Richness Using Reflectance and Texture Data Derived from QuickBird in a Recently Burned Area of Central Spain." *Remote Sensing of Environment* 119 (April): 208–21. https://doi.org/10.1016/j.rse.2011.12.024.
Wang, Ran, and John A. Gamon. 2019. "Remote Sensing of Terrestrial Plant Biodiversity." *Remote Sensing of Environment* 231 (September): 111218. https://doi.org/10.1016/j.rse.2019.111218.
Wang, Ran, John A. Gamon, Jeannine Cavender-Bares, Philip A. Townsend, and Arthur I. Zygielbaum. 2018. "The Spatial Sensitivity of the Spectral Diversity–Biodiversity Relationship: An Experimental Test in a Prairie Grassland." *Ecological Applications* 28 (2): 541–56. https://doi.org/10.1002/eap.1669.
Wang, Ran, John A. Gamon, Anna K. Schweiger, Jeannine Cavender-Bares, Philip A. Townsend, Arthur I. Zygielbaum, and Shan Kothari. 2018. "Influence of Species Richness, Evenness, and Composition on Optical Diversity: A Simulation Study." *Remote Sensing of Environment* 211 (June): 218–28. https://doi.org/10.1016/j.rse.2018.04.010.
Warren, Steven, Martin Alt, Keith Olson, Severin Irl, Manuel Steinbauer, and Anke Jentsch. 2014. "The Relationship between the Spectral Diversity of Satellite Imagery, Habitat Heterogeneity, and Plant Species Richness." *Ecological Informatics* 24. https://doi.org/10.1016/j.ecoinf.2014.08.006.
Woodcock, Curtis E., and Alan H. Strahler. 1987. "The Factor of Scale in Remote Sensing." *Remote Sensing of Environment* 21 (3): 311–32. https://doi.org/10.1016/0034-4257(87)90015-0.
Zhang, Yu, Han Y. H. Chen, and Anthony R. Taylor. 2016. "Aboveground Biomass of Understorey Vegetation Has a Negligible or Negative Association with Overstorey

Tree Species Diversity in Natural Forests." *Global Ecology and Biogeography* 25 (2): 141–50. https://doi.org/10.1111/geb.12392.
Zomer, R. J., A. Trabucco, and S. L. Ustin. 2009. "Building Spectral Libraries for Wetlands Land Cover Classification and Hyperspectral Remote Sensing." *Journal of Environmental Management* 90 (7): 2170–77. https://doi.org/10.1016/j.jenvman.2007.06.028.

Table 1. Spectral diversity indicators used in the study.

Spectral origin		**Calculation method**
		Statistical
		Mean
		Standard deviation (SD)
Bands	Blue	Range
	Green	Coefficient of variation (CV)
	Red	Mean distance from centroid (Distance)
	NIR	Unique value based
Vegetation index	NDVI	***S***
		H'
PCA	PC1	***D***
		J'
		$\boldsymbol{N_1}$
		$\boldsymbol{N_2}$

Table 2. The number of strong correlations between field diversity indices and spectral diversity indicators, and the strongest Pearson's correlation coefficient per resolution–extent combination.

Resolution	High		Low		Total number
Extent	Wide	Narrow	Wide	Narrow	
Number of strong correlations					
Canopy	4	5	11	59	79
Total	3	1	5	21	30
Pearson's correlation coefficient					
Canopy	0.36	- 0.36	0.36	0.50	
	S – NIR-$\boldsymbol{N_2}$	N_2 – PC1-CV	*S* – PC1-***D***	*J'* – PC1-***D***	
Total	- 0.44	0.34	0.40	0.50	
	H' – Blue-***J'***	*D* – Green-***J'***	*D* – PC1-***H'***	*J'* – PC1-***H'***	

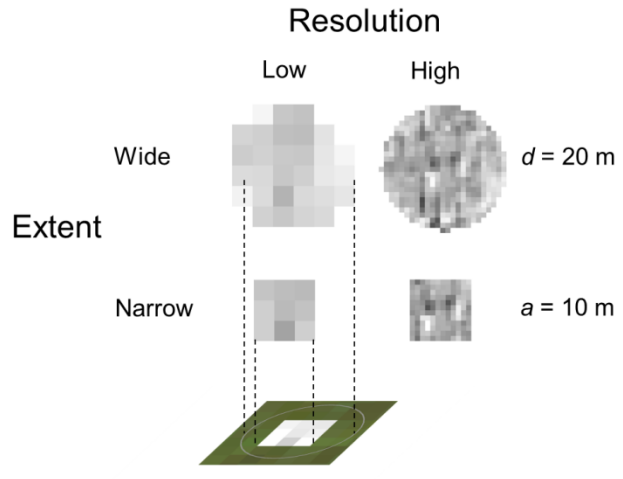

Figure 1. The four types of spectral plots used in the study, made by the combinations of low and high resolutions and narrow and wide extents. The field survey on forest canopy was carried out on a square plot (*a*, side = 10 m), corresponding to the low resolution–narrow extent spectral plot. The wide extent is marked by a circle (*d*, diameter = 20 m) with its centre in the middle of the plot established in the field.

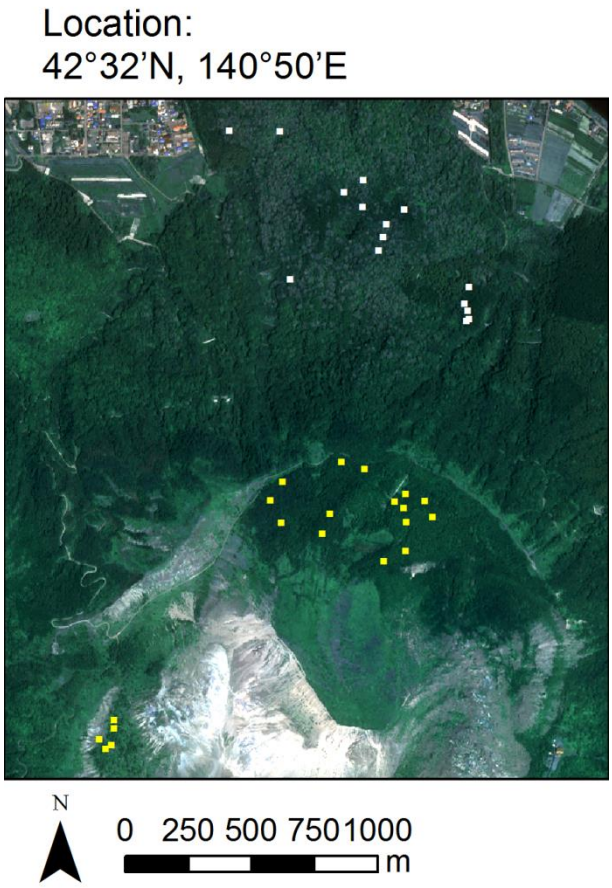

Figure 2. Locations of the 35 plots (10 m × 10 m) used for the study on Mount Usu, northern Japan. The white coloured plots cover mature forests, while the yellow plots are young forests, less than 110 and 40 years, respectively.

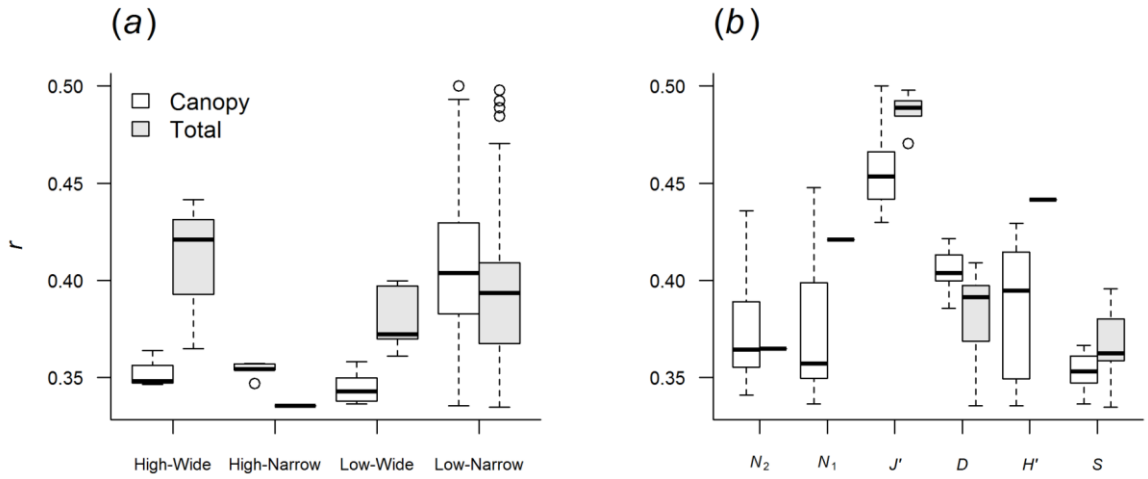

Figure 3. Box-whisker plots indicating the absolute values of Pearson's correlation coefficients (*r*) between spectral and field diversities depending on spectral resolution and extent (*a*) and on field indices used (*b*). Empty boxes indicate when spectral diversities are compared with canopy diversity and filled boxes when compared with total diversity. The field indices are abbreviated as N_2: true diversity of order 2, N_1: true diversity of order 1, *J'*: evenness, *D*: Gini-Simpson, *H'*: Shannon, and *S*: species richness.

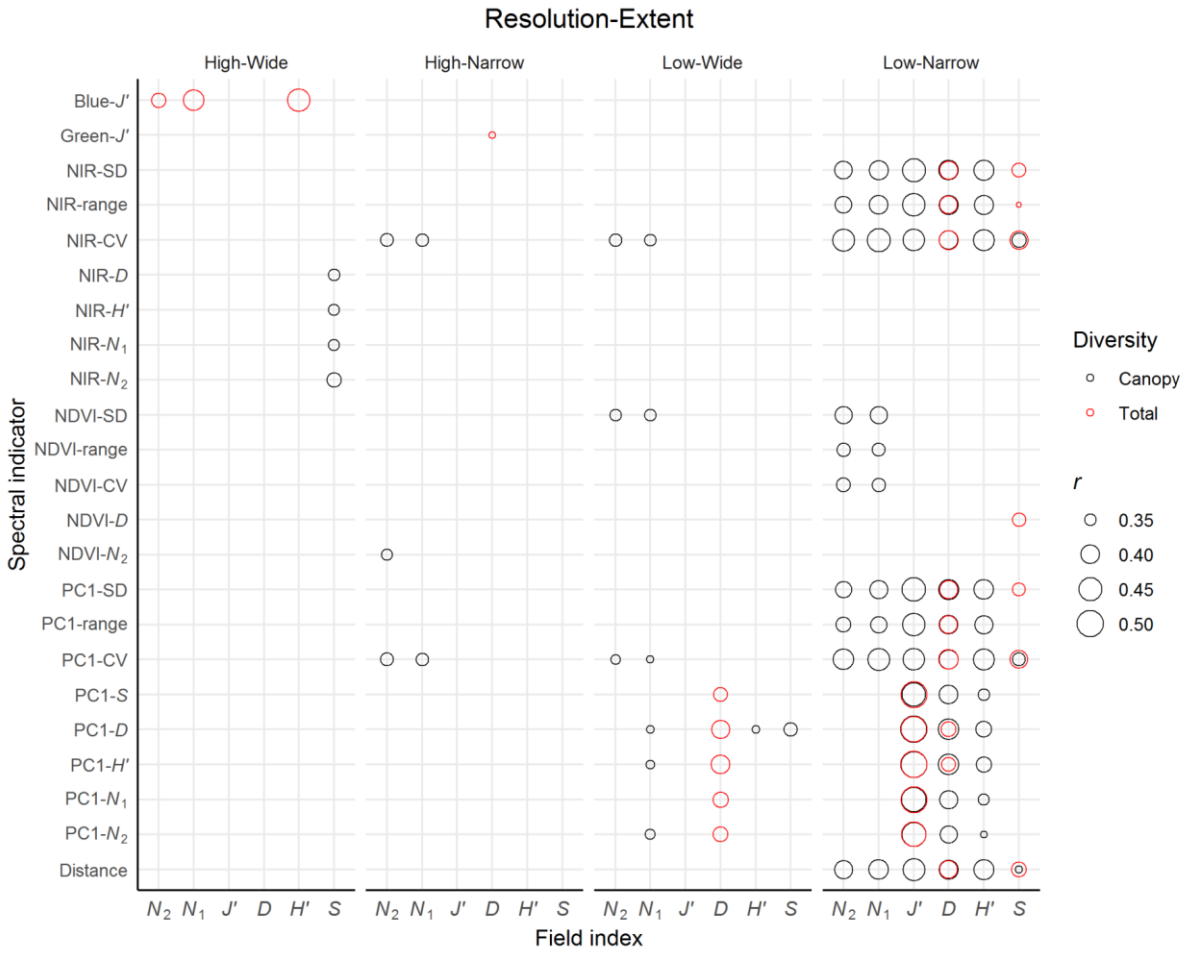

Figure 4. The absolute values of Pearson's correlation coefficients (*r*) between spectral diversities (*y* axis) and field indices (*x* axis) grouped by resolution and extent combinations. Black circles mark correlations with canopy diversities and red circles with total diversities. The size of the circles increases with increasing coefficients.

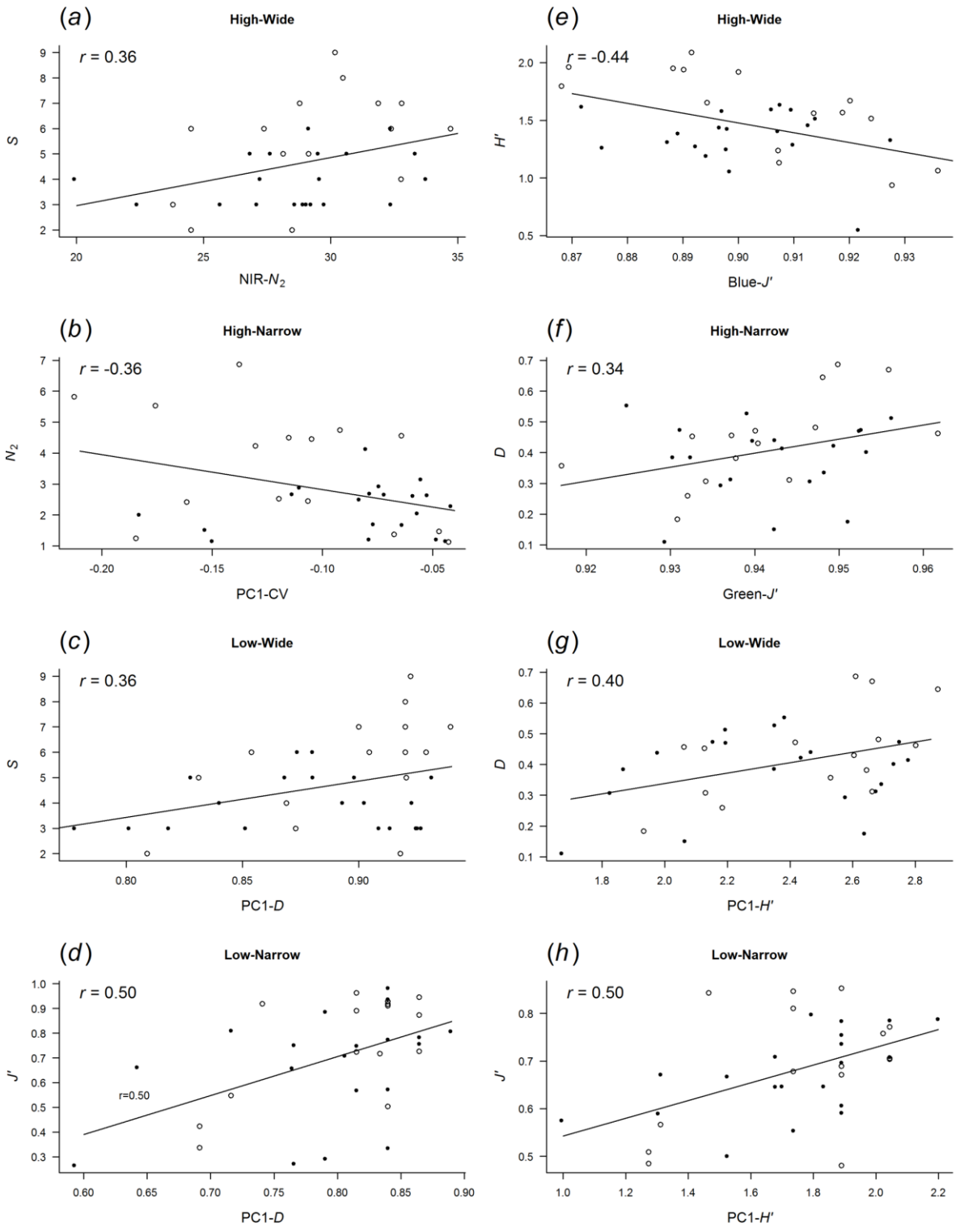

Figure 5. Pearson's correlation coefficients calculated from linear regressions between the best spectral indicators and canopy (*a-d*) and total diversity indices (*e-g*). The *x* axis shows the spectral indicators and the *y* axis shows the field diversities. Filled circles indicate young forest plots while empty circles indicate mature forest plots. All regressions are significant at $P < 0.05$.

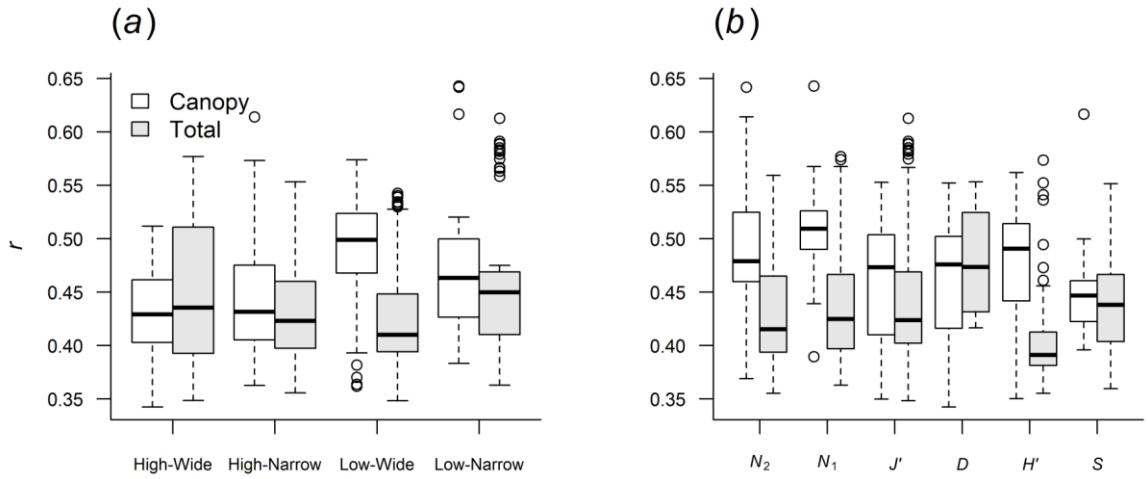

Figure 6. Regression between pairs of spectral indicators and field indices from the four resolution–extent combinations (*a*) and with different field indices (*b*). Empty boxes represent regression against canopy diversities and filled boxes against total diversities.

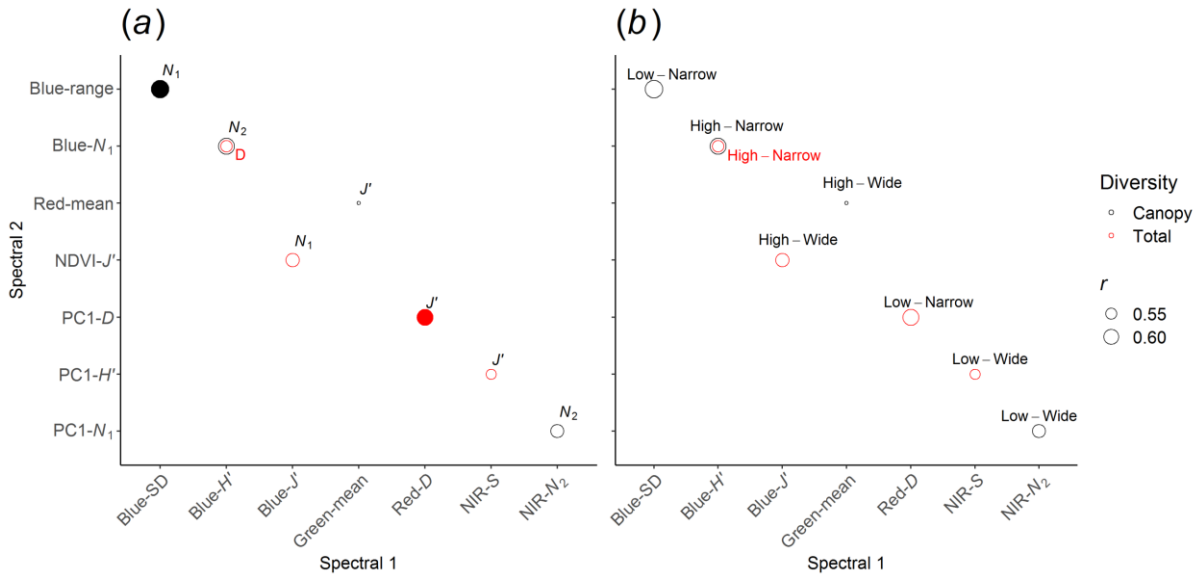

Figure 7. Best spectral indicator pairs to estimate field diversities (*a*) and the resolution–extent combination they are calculated from (*b*). The field diversities estimated with the highest accuracy are marked by filled circles on the left plot.